

Multi-temporal analysis of land use and land cover change detection in Binh Duong province, Vietnam using geospatial techniques

Bui Bao Thien^{1*}, Vu Thi Phuong²

¹Southern Federal University, Rostov-on-Don, Russia

e-mail: buibaothienha@gmail.com; ORCID: <http://orcid.org/0000-0003-2964-0012>

²Hong Duc University, Thanh Hoa, Vietnam

e-mail: vuthiphuong@hdu.edu.vn; ORCID: <http://orcid.org/0000-0001-9277-2013>

*Corresponding author: Bui Bao Thien, e-mail: buibaothienha@gmail.com

Received: 2023-09-19 / Accepted: 2024-06-25

Abstract: Understanding changes in land use and land cover (LULC) is crucial for effective land management, environmental planning, and decision-making. It helps identify areas of environmental concern, assess the impacts of human activities on ecosystems, and develop strategies for conservation efforts and sustainable land use. In this study, remote sensing and geographic information systems (GIS) were used to monitor LULC changes in Binh Duong province, Vietnam from 1988 to 2023. The supervised classification method in ArcGIS 10.8 software was applied to Landsat satellite data (Landsat 5-TM for 1988 and 2004, and Landsat 9-OLI/TIRS for 2023) to detect and classify five main LULC types: arable land, barren land, built-up areas, forests and waterbodies. The classification accuracy was evaluated using kappa coefficients, which were 0.877, 0.894 and 0.908 for 1988, 2004, and 2023, respectively. During the period of 1988–2023, the forest, barren land, and waterbodies class areas decreased by 560.55 km², 200.04 km², and 19.68 km², respectively. Meanwhile, the arable land and built-up areas classes increased by 343.80 km² and 436.47 km², respectively. Furthermore, the Normalized Difference Vegetation Index (NDVI) and the Normalized Difference Built-up Index (NDBI) were used to quickly assess changes in LULC, and their trends were found to be consistent with the supervised classification results. These changes in LULC pose significant threats to the environment and the findings of this study can serve as valuable resources for future land management and planning in the region.

Keywords: Landsat, land management, vegetation index, remote sensing, maximum likelihood classification



The Author(s), 2024 Open Access. This article is distributed under the terms of the Creative Commons Attribution 4.0 International License (<http://creativecommons.org/licenses/by/4.0/>), which permits unrestricted use, distribution, and reproduction in any medium, provided you give appropriate credit to the original author(s) and the source, provide a link to the Creative Commons license, and indicate if changes were made.

1. Introduction

Land use refers to the purposeful utilization of land resources as indicated by the land surface cover, under the influence of human activities or land managers, pertaining to the issue of exploiting land surface cover (Msofe et al., 2019; Angessa et al., 2021; Thien et al., 2022). This reflects human activities such as creation of industrial zones, residential areas, farmlands, grasslands, timber extraction, mineral extraction, and other various endeavors (Rajkhowa et al., 2021). Moreover, land cover is defined as an essential element of the Earth's ecosystem, playing a key role in many areas, including shaping climate, hydrology, biogeochemical cycles, maintaining biodiversity and resources, as well as playing a key role in integrated interactions between human activities and the environment (Právělie, 2018; Kumari et al., 2019; Fisher and Koven, 2020). Changes in land surface cover involve alterations to Earth's surface due to human activities, although natural factors can also contribute to these changes (Awotwi et al., 2018). These alterations signify significant surface transitions and are pivotal factors driving environmental degradation within any landscape. Land use and land cover (LULC) changes have evolved into a fundamental and central component of present strategies aimed at natural resource management and addressing environmental transformations (Heredia-R et al., 2021; Regasa et al., 2021).

Currently, the study of LULC dynamics has become more convenient with the support of remote sensing and geographic information systems (GIS) (Aboelnour and Engel, 2018; Zadbagher et al., 2018; Thien et al., 2023b). Remote sensing data is characterized by its multi-temporal nature, fast processing and wide coverage, which serves as an effective tool for accurate and rapid monitoring of LULC changes (Adegboyega, 2021). The utilization of remote sensing imagery and GIS also allows for adjustments and supplementation of necessary data that cannot be feasibly acquired through on-site investigation, surveying, and measurement during the local land use planning and adjustment process. For LULC planners, Landsat sensors play a pivotal role by providing a wealth of satellite data, particularly in detecting changes in the Normalized Difference Built-up Index (NDBI), Normalized Difference Vegetation Index (NDVI), and LULC categories (Slamet et al., 2021; Waiyasusri, 2021; Thien and Phuong, 2023). Detection of changes related to the utilization of remote sensing information enables the quantification of previous impacts resulting from a single occurrence, thus supporting the tracking of LULC attribute changes with reference to various satellite data sources. Supervised classification demands prior knowledge about scene categories and regions containing relevant materials, training locations, storage, and outlining for use within the supervised classification algorithm (Moharram and Sundaram, 2023; Thien et al., 2023b).

The dynamics of LULC changes on a global scale, as well as in Vietnam, are becoming significant and challenging issues in the current era (Hanh et al., 2017; Rimal et al., 2018; Niu et al., 2022). Throughout the processes of economic development, and population growth, the intricate interaction between humans and the environment has contributed to notable alterations in the structure of land use and land cover. Globally, the expansion of urban areas, the development of industrial zones, and the expansion of agricultural regions have led to a transformation of land area from arable to urban and industrial uses (Rustiadi et al., 2021). This often coincides with a reduction in forested and wildland areas, resulting

in issues related to ecological decline, habitat loss for wildlife and wild plants, and increased susceptibility to natural disasters such as floods and landslides. In Vietnam, with rapid economic and population growth, changes in land use are also occurring swiftly (Fox and Vogler, 2005; Vadrevu et al., 2019). The urbanization trend, increased agricultural and industrial production, along with shifts from traditional land use patterns, have significantly altered the structure of LULC. However, challenges such as sustainable land resource management, environmental protection, and maintaining a balance between economic development and nature conservation are also emerging. Recognizing the importance of maintaining sustainable LULC, careful management strategies and monitoring are necessary to ensure that economic development does not irreversibly harm land resources and the natural environment (Motlagh et al., 2020; Wu et al., 2022).

Many previous studies have been performed worldwide on LULC, primarily aiming to grasp the intricate dynamics of land and its transformations concerning build-up areas, forests, water bodies, arable land, and the broader environmental terrain over time and space (Aboelnour and Engel, 2018; Zadbagher et al., 2018; Slamet et al., 2021; Waiyasusri, 2021; Thien and Phuong, 2023; Thien et al., 2023a). In recent years, the widespread adoption of advanced remote sensing and GIS has emerged as an invaluable asset for comprehensively assessing the spatial and temporal aspects of landscape dynamics, thereby aiding in the evaluation of global-scale changes across diverse terrains (Zadbagher et al., 2018; Slamet et al., 2021; Thien et al., 2023b). Despite the extensive body of research, crucial aspects such as the trends, extent, and magnitude of LULC modifications within specific research frameworks have often been overlooked. Consequently, a comprehensive understanding of the degree of change, the underlying driving forces, and their ramifications remains elusive. This study seeks to address these gaps by employing an integrated approach utilizing the NDVI and NDBI to analyze and elucidate the driving factors and consequences contributing to LULC dynamics. Studying LULC dynamics in Binh Duong province provides valuable insights for local stakeholders and global researchers and policymakers, especially in Europe, where similar urbanization, industrialization, and agricultural expansion occur (Malinowski et al., 2020; Gozdowski et al., 2022; Mingarro and Lobo, 2023; Gadal and Gloaguen, 2023). By comparing our findings with studies in Europe, we can identify common challenges and strategies for sustainable land management. This research contributes to both local understanding and global efforts to address landscape transformation. Moreover, this research endeavors to contribute to filling the existing scientific void in the realm of land management in Vietnam, thereby offering valuable insights to aid in informed decision-making processes.

In the present work, the changing pattern of LULC in Binh Duong province, Vietnam from 1988 to 2023 has been mapped using multitemporal satellite images from Landsat 5-TM and Landsat 9-OLI/TIRS imagery. The main objective of this study was to assess the trend of LULC change in the study area. Tasks of research: (1) identify and classify LULC types and to quantitatively analyze LULC changes from 1988 to 2023; (2) then conduct NDVI and NDBI change detection, mapping and analysis using satellite data; and (3) identify and describe impact of the factors affecting the changes of LULC in the study area in the period 1988–2023.

2. Material and methods

2.1. Study area

Binh Duong province, located in the South of Vietnam, is located in geographical coordinates with latitude $10^{\circ}35'N$ – $11^{\circ}15'N$ and longitude $106^{\circ}24'E$ – $107^{\circ}10'E$, with a total area of $2,694.64 \text{ km}^2$ (Fig. 1) (Binh Duong Statistics Office, 2022). This province borders with Dong Nai province, Tay Ninh province, Binh Phuoc province and Ho Chi Minh city, about 30 km north of Ho Chi Minh city. The region's landscape is diverse, featuring plains, hills, and riverside areas. Around 40% of the province's land area consists of plains, while the remaining 60% encompasses hilly terrain and rivers. The province's climate is characterized as tropical monsoon, with distinct wet and dry seasons. The average annual temperature hovers around $27^{\circ}C$, and the region experiences approximately 2,500 to 2,700 hours of sunlight annually. As of the latest data available, the province's population, as reported in the Binh Duong statistical yearbook, was approximately 2,685,513 people in 2021 (Binh Duong Statistics Office, 2022). Urban population accounts for about 83.42% of this population, residing in cities, towns and industrial zones, the rest of the rural population accounts for 16.58%. Binh Duong province is a key industrial hub in Vietnam, known for its robust economic growth and rapid urbanization. The gross domestic product (GDP) per capita in 2020 was \$4,573, with the economy primarily driven by the manufacturing and construction sectors. Agriculture and services sectors also play significant roles in the province's economy. The province is home to numerous industrial parks and export processing zones, attracting both domestic and foreign investments.

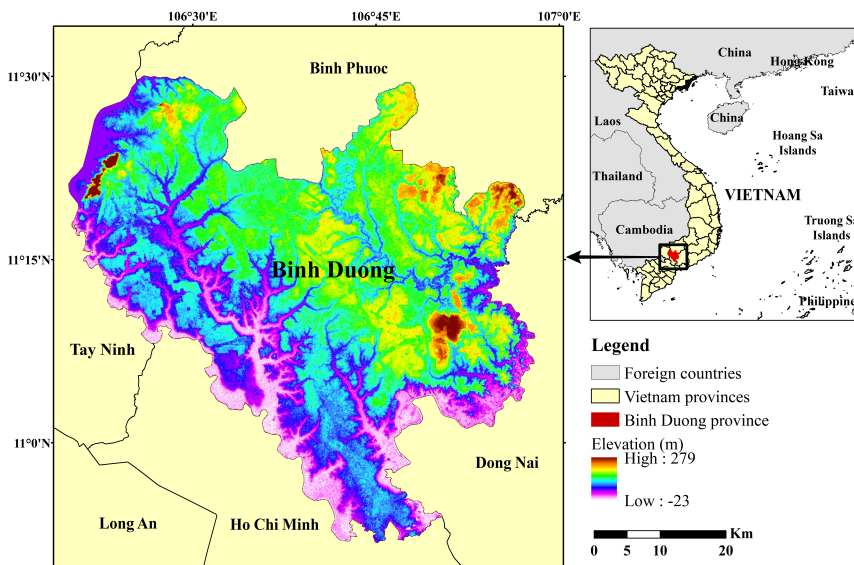


Fig. 1. Map of study area, Binh Duong province, Vietnam

2.2. Data collection

Satellite images were used to map LULC in Binh Duong province from 1988 to 2023 and assess changes in LULC. Landsat 5-TM images were used for the years 1988 and 2004 and Landsat 9-OLI/TIRS images were used for 2023 in this study. The Landsat images with a path/row of 125/052 were downloaded from the USGS Glovis websites (<https://glovis.usgs.gov>). A detailed data summary is given in Table 1. In addition, point data with 300 points per year were collected to evaluate the accuracy of the LULC classification map. For 1988 and 2004, these points data were collected using Google Earth Pro software. For 2023, field surveys used GPS to record precise coordinates of different land cover types. To ensure robust validation, the collected field data were cross-referenced with other available geospatial datasets, such as high-resolution aerial imagery, cadastral maps, and land use inventories if applicable. By comparing and correlating field measurements with these supplementary geodata sources, researchers could verify the consistency and reliability of the LULC classification results derived from satellite imagery. Throughout the study, ArcGIS 10.8 and Microsoft Excel 2016 software were used.

Table 1. Detailed data summary of satellite imagery used in the study

Satellite image	Sensor	Acquisition data	Cloud cover land	Landsat scene ID
Landsat 5	TM	14/01/1988	0.00	LT51250521988014BKT00
Landsat 5	TM	11/02/2004	3.00	LT51250522004042BKT00
Landsat 9	OLI/TIRS	23/02/2023	0.73	LC91250522023054LGN01

2.3. Image pre-processing and supervised classification

To acquire a comprehensive image of the study area, distinct bands from Landsat 5-TM and Landsat 9-OLI/TIRS were combined using layer stacking (Mehdi et al., 2016; Thien et al., 2023b). The desired study area was delineated using extract by mask tools within ArcGIS 10.8 during the subset setup process (Wahla et al., 2023). Referring to the scheme proposed by Anderson et al. (1976) and confirmed through field surveys in the study area, five primary LULC categories were identified, encompassing arable land, barren land, built-up areas, forests, and waterbodies (Table 2). From the predetermined LULC categories, polygons were drawn around pixels with common reflectance values for each category, creating a training sample within ArcGIS 10.8 software (Thien and Phuong, 2023). Pixels enclosed by these polygons in each Landsat image were marked to generate spectral signatures for different LULC classes. Subsequently, a maximum likelihood classification algorithm was applied to classify LULC based on these spectral signatures (Verma et al., 2020). Figure 2 provides a detailed illustration of the methodology employed in this research.

Table 2. Classes delineated from field survey

Class	Description
Arable land	Cropland and paddy field
Barren land	Fallow land, sands and earth dumps
Built-up areas	Residential areas, industrial, roads and other manmade structures
Forests	Natural forest, plantations and mixed forest lands
Waterbodies	Reservoirs, rivers and lakes

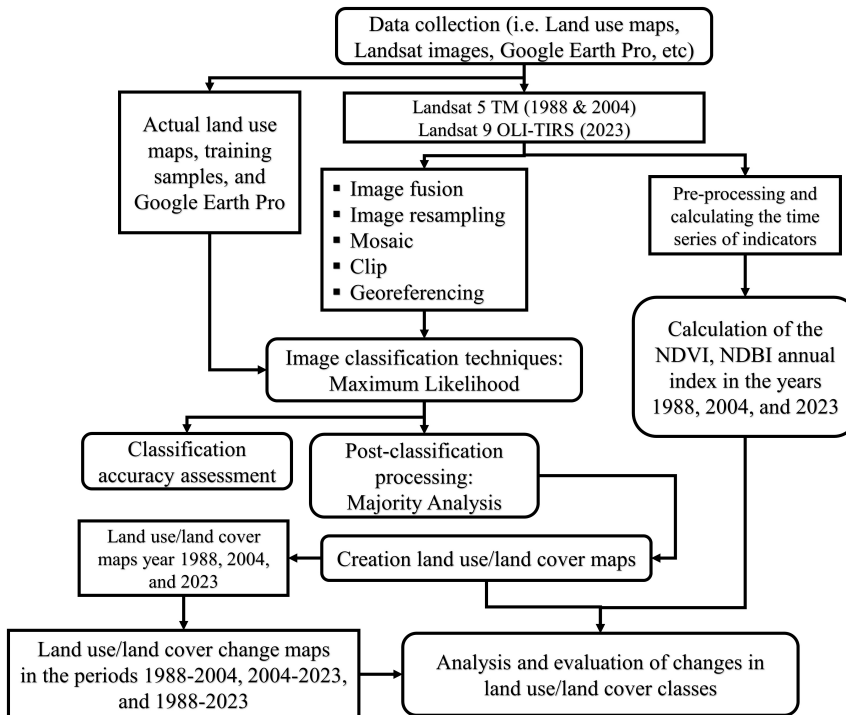


Fig. 2. Flow chart for methodology

2.4. Classification accuracy assessment

In the process of LULC classification, it is possible to have misclassifications between pixels, so it is necessary to evaluate the accuracy after classification (Theres and Selvaku-mar, 2022; Dash et al., 2023). The accuracy of the classification results is assessed using an error matrix, which compares the results with 150 reference data points collected for each year. User’s accuracy, producer’s accuracy, overall accuracy, and kappa coefficient are computed based on the error matrix for each respective year (Foody, 2020; Islami et al., 2022). The kappa coefficient serves as a measure of reliability for the classification,

indicating the agreement between the predicted and actual classification results. User's accuracy, producer's accuracy, overall accuracy, and kappa coefficient are calculated using formulas (1), (2), (3), and (4), respectively:

$$\text{User's accuracy} = \frac{\text{Number of correctly classified pixels in each category}}{\text{Total number of reference pixels in each category (row total)}} \times 100, \quad (1)$$

$$\text{Producer's accuracy} = \frac{\text{Number of correctly classified pixels in each category}}{\text{Total number of reference pixels in each category (column total)}} \times 100, \quad (2)$$

$$\text{Overall accuracy} = \frac{\text{Number of sampling classes classified correctly}}{\text{Number of reference sampling classes}} \times 100, \quad (3)$$

$$\text{Kappa} = \frac{P_o - P_e}{1 - P_e}, \quad (4)$$

where P_o is the agreement ratio between the predicted classification results and the actual classification results. P_e is the random agreement ratio between the predicted classification results and the actual classification results.

2.5. Estimation and correlation between NDVI and NDBI

The estimation of NDVI and NDBI from satellite imagery provides valuable information for monitoring the health of vegetation and urbanization processes (Rouse et al., 1973; Slamet et al., 2021; Waiyasusri, 2021; Singh et al., 2022). NDVI serves as a vegetation index, utilizing the distinction between the near-infrared (NIR) and red (RED) bands of satellite images. The NDVI value increases as vegetation cover expands and decreases as vegetation cover diminishes (Rouse et al., 1973; Dutta et al., 2021). On the other hand, NDBI serves as an urban index, utilizing the difference between the shortwave infrared (SWIR) and near-infrared (NIR) bands of satellite images. The NDBI value increases with the expansion of built-up areas and decreases as the built-up area decreases (Chatterjee and Majumdar, 2022). The calculation of the NDVI and NDBI indices are performed using formulas (5) and (6) respectively.

$$\text{NDVI} = \frac{\text{NIR} - \text{RED}}{\text{NIR} + \text{RED}}, \quad (5)$$

$$\text{NDBI} = \frac{\text{SWIR} - \text{NIR}}{\text{SWIR} + \text{NIR}}. \quad (6)$$

Regression analysis was used to measure the correlation between NDVI and NDBI in Binh Duong province for the years 1988, 2004 and 2023. The correlation coefficient values generated by the regression analysis range from -1 to +1 (Pal and Ziaul, 2017). To perform the regression analysis, 200 random point data were generated within the study area boundaries using the random point generator in ArcGIS 10.8 software. The extract multi values to points tool was used to extract a value for each point data from the NDVI and NDBI pixels. These values were exported to Excel 2016 software (Microsoft, USA) to estimate the regression equation between NDVI and NDBI.

3. Results and discussio

3.1. Land use/land cover classification

The map of LULC status in Binh Duong province in the three years 1988, 2004 and 2023 is shown in Figure 3. Table 3 shows the area and proportions of each LULC type respectively. From Figure 3 and the data in Table 3, it can be seen that significant changes have occurred in arable land and built-up classes over the 35 years in the study area.

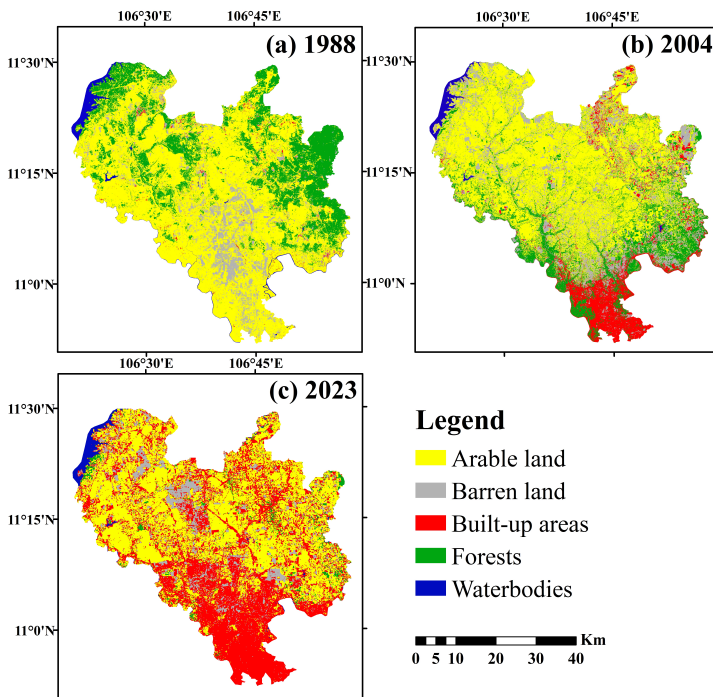


Fig. 3. Land use/land cover maps for Binh Duong province in 1988 (a), 2004 (b), and 2023 (c)

Based on the LULC classification results in Table 3, in the year 1988, arable land class accounted for the largest area in Binh Duong province, constituting 64.48% (1737.43 km²) of the total area. Forests area accounted for 23.40% (630.60 km²), barren land area accounted for 9.09% (244.94 km²), waterbodies class area accounted for 2.02% (54.36 km²), and built-up class area had the smallest coverage at only 1.01% (27.31 km²) (Table 3). By 2004, the areas of arable land, forests, and waterbodies classes had decreased to 55.45% (1494.07 km²), 17.06% (459.62 km²), and 1.32% (35.67 km²), respectively (Table 3). In contrast, the areas of barren land and built-up classes had increased to 16.75% (451.26 km²) and 9.43% (254.02 km²), respectively (Table 3). By 2023, the area of arable land class had further increased and accounted for 77.24% (2081.23 km²). Additionally, the area of built-up class had continued to rise and accounted for 17.21% (463.78 km²) in 2023. Meanwhile, the areas of barren land, forests, and waterbodies

classes had decreased to 1.67% (44.90 km²), 2.60% (70.05 km²), and 1.29% (34.68 km²), respectively (Table 3). From the classification results, it can be observed that in 1988, the majority of the forests class was distributed in the northwest and southeast directions. The arable land class was distributed adjacent to the forests class. By 2004, a concentrated built-up area appeared in the southern region of Binh Duong province, with the forests class surrounding it. By 2023, the built-up area had expanded, leading to the loss of the forests class. These changes reflect the ongoing urbanization and agricultural expansion processes taking place in the province, a pattern akin to what has been observed in many European countries. Urbanization and industrialization there have similarly led to the expansion of built-up areas at the expense of natural habitats such as forests and wetlands (Malinowski et al., 2020; Mingarro and Lobo, 2023). This trend is often driven by similar factors, including population growth, economic development, and infrastructure projects. Studies in Europe may also highlight the importance of policy interventions and land use planning in shaping LULC dynamics, as well as the challenges associated with balancing economic growth with environmental conservation. Furthermore, in the Baltic States and Poland, agricultural expansion and intensification have historically been significant drivers of LULC change, leading to the conversion of forests and grasslands into arable land (Wiatkowska et al., 2021; Kovyazin et al., 2023). However, in recent years, there has been an increasing recognition of the need for sustainable land management practices to mitigate the environmental impacts of agriculture and preserve biodiversity (Gozdowski et al., 2022; Balawejder et al., 2023; Gadai and Gloaguen, 2023).

Table 3. The land use/land cover area distribution from 1988 to 2023 in Binh Duong province

Class	1988		2004		2023	
	Area (km ²)	(%)	Area (km ²)	(%)	Area (km ²)	(%)
Arable land	1737.43	64.48	1494.07	55.45	2081.23	77.24
Barren land	244.94	9.09	451.26	16.75	44.90	1.67
Built-up	27.31	1.01	254.02	9.43	463.78	17.21
Forest	630.60	23.40	459.62	17.06	70.05	2.60
Waterbodies	54.36	2.02	35.67	1.32	34.68	1.29
Total	2694.64	100.00	2694.64	100.00	2694.64	100.00

The assessment of the post-classification accuracy in this study was performed by comparing the classified LULC classes with the reference data (Singh et al., 2014; Chughtai et al., 2021). The results of the classification evaluation showed that the overall accuracy of the years 1988, 2004 and 2023 was 90.67%, 92.00% and 93.33%, respectively (Table 4). Overall, the producer's accuracy and the user's accuracy for each soil layer in all 3 years were above 80% (Table 4). The kappa coefficient values in 1988, 2004 and 2023 in the study area were recorded as 0.877, 0.894 and 0.908, respectively (Table 4). Kappa coefficients ranging from 0.81 to 1.00 are considered almost perfect in LULC classification (Rivière et al., 2018). These results show reliable land cover classification and good consistency between referenced and classified maps.

Table 4. Accuracy assessments for classified maps

LULC classes	1988		2004		2023	
	Producer's accuracy (%)	User's accuracy (%)	Producer's accuracy (%)	User's accuracy (%)	Producer's accuracy (%)	User's accuracy (%)
Arable land	90.74	92.45	92.98	94.64	93.10	94.74
Barren land	91.67	89.19	91.43	94.12	84.62	91.67
Built-up areas	86.67	86.67	86.96	95.24	97.87	95.83
Forests	92.59	89.29	95.00	86.36	84.62	84.62
Waterbodies	88.89	94.12	93.33	82.35	94.74	90.00
Overall accuracy (%)	90.67		92.00		93.33	
Kappa Coefficient	0.877		0.894		0.908	

3.2. Land use/land cover change

Figure 4 illustrates the specific changes in each LULC class during three periods (1988–2004, 2004–2023, and 1988–2023) in Binh Duong province. The analysis of the area changes for each LULC class during these periods is also presented in Table 5. During the period 1988–2004, the arable land area showed the highest decrease, accounting for 9.03% (243.36 km²) compared to the initial area. The forest and waterbodies areas also decreased by 6.35% (170.98 km²) and 0.69% (18.69 km²), respectively. Conversely, the built-up and barren land areas showed significant increases, with 8.41% (226.71 km²) and 7.66% (206.32 km²), respectively. Examining the LULC change pattern during the period 2004–2023, it can be observed that the arable land area increased by 21.79% (587.16 km²). Along with that, the built-up area continued to expand by 7.78% (209.76 km²). Meanwhile, the forest and waterbodies areas experienced further decreases during the period 2004–2023, with 14.46% (389.57 km²) and 0.04% (0.99 km²), respectively (Table 5). Additionally, during the period 2004–2023, the barren land area decreased significantly compared to the increasing trend observed in the period 1988–2004, with a total reduction of 15.08% (406.36 km²) (Table 5).

Table 5. The land use/land cover change analysis from 1988 to 2023 in Binh Duong province

Class	1988–2004		2004–2023		1988–2023	
	Area (km ²)	(%)	Area (km ²)	(%)	Area (km ²)	(%)
Arable land	–243.36	–9.03	587.16	21.79	343.80	12.76
Barren land	206.32	7.66	–406.36	–15.08	–200.04	–7.42
Built-up areas	226.71	8.41	209.76	7.78	436.47	16.20
Forests	–170.98	–6.35	–389.57	–14.46	–560.55	–20.80
Waterbodies	–18.69	–0.69	–0.99	–0.04	–19.68	–0.73

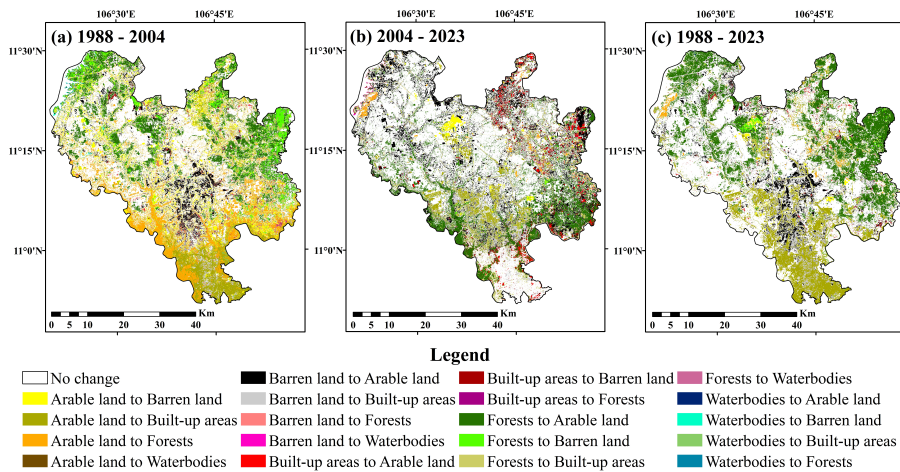


Fig. 4. Land use/land cover changes maps for Binh Duong province in 1988, 2004, and 2023

In general, in the past 35 years (1988–2023) in the study area, there have been notable changes in LULC. From Figure 4 and Table 5, it is shown that the built-up area has steadily increased by 16.20% (436.47 km²) and became prominent in Binh Duong province in the period 1988–2023. The main reason for this expansion is the successful development of industrial zones and clusters, which has created a demand for labor and led to an increase in the influx of migrant workers. The growing population, both from migration and local residents, has resulted in an increased demand for residential land and housing construction (Sokolov et al., 2019; Surya et al., 2021). By 2023, additional residential areas have been established to accommodate the resettlement needs of households affected by provincial development projects. These residential areas also cater to the housing needs of industrial workers, production clusters, and the demand for separate households (Lenzen et al., 2006). In contrast, most of the forests area was converted to other LULC with 20.80% (560.55 km²) (Table 5). Meanwhile, the area of arable land and barren land has increased and decreased differently between the two periods (1988–2004 and 2004–2023). Overall over the past 35 years, the area of arable land has increased by 12.76% (343.80 km²), and the area of barren land has decreased by 7.42% (200.04 km²) (Table 5). The main reason for the significant reduction in unused land is the conversion of barren land for arable land. Additionally, the arable land class also started encroaching on the forested areas. The development of irrigation systems in the Dong Nai river basin has provided proactive water resources for irrigation, enabling people to exploit previously unused land for agricultural purposes (Bo et al., 2019). The area of water bodies in the period 1988–2023 decreased by 0.73% (19.68 km²) (Table 5).

3.3. The NDVI and NDBI

The high NDVI index values indicate denser and healthier vegetation, while lower values correspond to sparse or no vegetation (Rouse et al., 1973; Rousta et al., 2020; Lemenkova and Debeir, 2023). In 1988, the NDVI value ranged from –0.46 to +0.69 (Fig. 5a); in 2004,

NDVI values ranged from -0.51 to $+0.74$ (Fig. 5b); and in 2023, NDVI values ranged from -0.36 to $+0.62$ (Fig. 5c). Significant spatial changes in vegetation cover and green area were observed between the lowest and highest NDVI values recorded in 2004, along with improved agricultural productivity in areas such as forests and vegetation cover (Figs. 5a,b,c). The NDBI index is used to assess the level of urban development in the study area, the NDBI values increase as the built-up area increases and decreases when the built-up area decreases (Zheng et al., 2021; Chatterjee and Majumdar, 2022). In 1988, the NDBI value ranged from -0.57 to $+0.74$ (Fig. 5d); in 2004, NDBI values ranged from -0.83 to $+0.65$ (Fig. 5e); and in 2023, the NDBI values ranged from -0.47 to $+0.65$ (Fig. 5f) The red areas in Figures 5d,e and 5f show minimal vegetation cover, such as built-up and barren land.

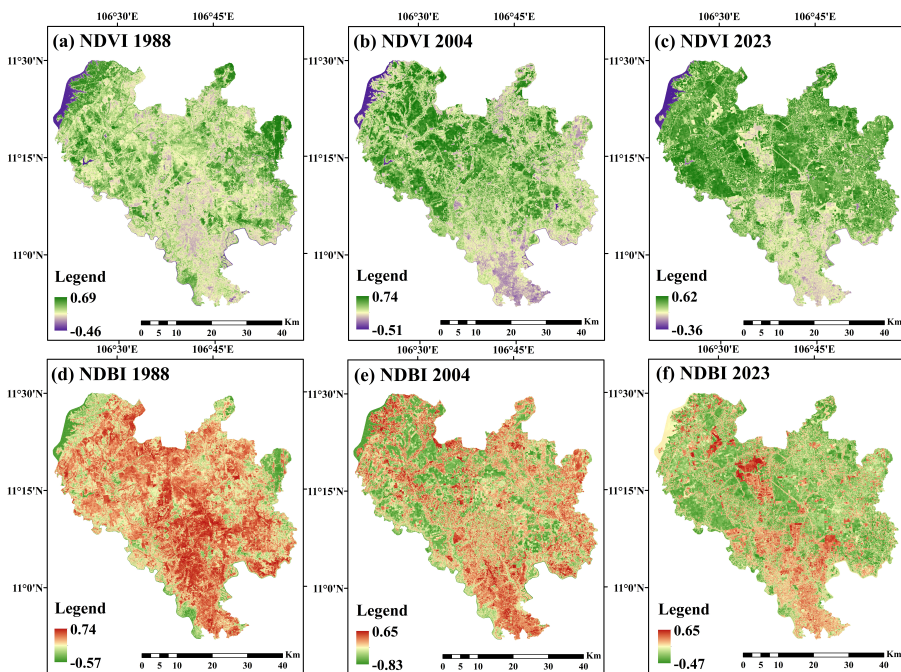


Fig. 5. NDVI and NDBI maps for Binh Duong province in 1988, 2004, and 2023

A linear regression analysis was conducted to demonstrate the relationship between two indices (NDVI and NDBI) (Florim et al., 2021). The changes in NDBI values related to land use were assessed by evaluating the variations in land use intensity within the LULC units through regression analysis (R^2) (Majeed et al., 2021). Furthermore, a negative correlation between NDVI and NDBI was identified. Specifically, correlation coefficients of $R^2 = 0.7249$ for 1988, $R^2 = 0.8001$ for 2004, and $R^2 = 0.7799$ for 2023 were depicted in Figure 6. As observed in Figure 6, this illustrates the relationship between the vegetation index (NDVI) and the integrated component derived from NDBI. The regression analysis also revealed that the highest NDBI values corresponded to areas with the lowest NDVI values, and vice versa. This clearly indicates that the increase in built-up areas and barren land leads to a decrease in vegetation coverage.

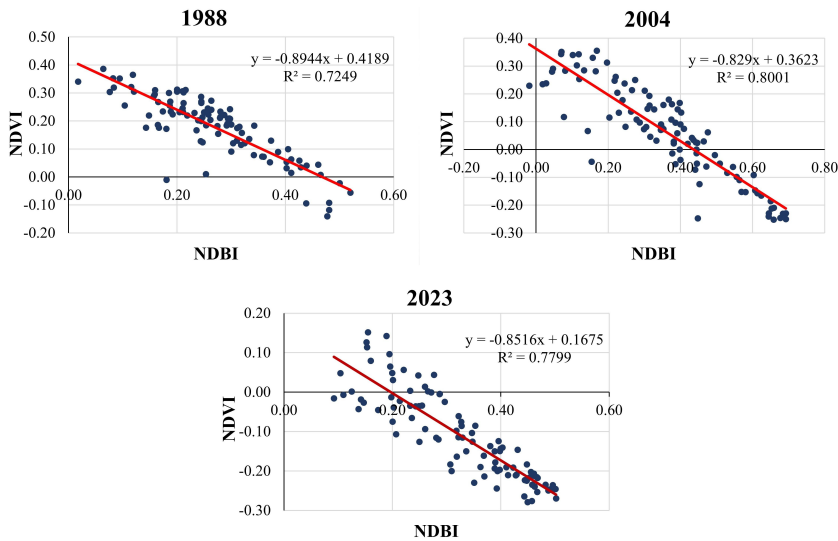


Fig. 6. Regression analyses between NDVI and NDBI in Binh Duong province

4. Conclusion

Our research used remote sensing and GIS to map LULC, thus detecting and evaluating the level of change in LULC in Binh Duong province, Vietnam, from 1988 to 2023, to better understand the LULC change process. Over the 35-year period, the study area has experienced a decline in forests, barren land, and waterbodies classes, with area decreases of 20.80%, 7.42%, and 0.73%, respectively. Additionally, there has been a substantial increase in the extent of arable land and built-up class areas from 1988 to 2023, with a total increase of 12.76% and 16.20%, respectively. The NDVI and NDBI indices were also employed to evaluate changes in land cover characteristics, revealing a strong correlation between impervious surfaces and vegetation cover. Forested land may continue to decrease due to population growth, human settlement, poverty, and the demand for arable land to meet the needs of the local population in the study area. The results show that the reduction of forested areas and the expansion of arable land and built-up areas over the past 35 years reflect human activities influenced by national and local policies, leading to deforestation, loss of forest biodiversity, and decreased ecosystem services in the study area. Addressing deforestation, forest degradation, urban expansion, construction, arable land conversion, and the loss of wetlands and water bodies in the study area requires urgent intervention from forest managers, environmentalists, decision-makers, and other stakeholders.

Author contributions

Conceptualization: B.B.T.; collection and assembly of data: B.B.T., V.T.P.; data analysis and interpretation: B.B.T., V.T.P.; writing the article: B.B.T.; critical revision of the article: B.B.T.; final approval of the article: B.B.T., V.T.P.

Data availability statement

The data used to support the findings of this study are available from the corresponding author upon reasonable request.

Acknowledgements

This research received no external funding. The authors would like to thank the anonymous reviewers for their thoughtful comments and efforts toward improving our manuscript.

References

- Aboelnour, M., and Engel, B.A. (2018). Application of remote sensing techniques and geographic information systems to analyze land surface temperature in response to land use/land cover change in Greater Cairo Region. *Egypt. J. Geogr. Inf. Syst.*, 10(1), 57–88. DOI: [10.4236/jgis.2018.101003](https://doi.org/10.4236/jgis.2018.101003).
- Adegboyega, S.A.A. (2021). Multi-temporal land use/land cover change detection and urban watershed degradation in Olorunda Local Government Area, Osun State, Nigeria. *Appl. Geomat.*, 13(4), 659–676. DOI: [10.1007/s12518-021-00382-3](https://doi.org/10.1007/s12518-021-00382-3).
- Anderson, J.R., Hardy, E.E., Roach, J.T. et al. (1976). *A land use and land cover classification system for use with remote sensor data*. Geological survey professional paper, U.S. government printing office. Washington DC, 964, 1–28.
- Angessa, A.T., Lemma, B., and Yeshitela, K. (2021). Land-use and land-cover dynamics and their drivers in the central highlands of Ethiopia with special reference to the Lake Wanchi watershed. *GeoJournal*, 86(3), 1225–1243. DOI: [10.1007/s10708-019-10130-1](https://doi.org/10.1007/s10708-019-10130-1).
- Awotwi, A., Anornu, G.K., Quaye-Ballard, J.A. et al. (2018). Monitoring land use and land cover changes due to extensive gold mining, urban expansion, and agriculture in the Pra River Basin of Ghana, 1986–2025. *Land Degrad. Dev.*, 29(10), 3331–3343. DOI: [10.1002/ldr.3093](https://doi.org/10.1002/ldr.3093).
- Balawejder, M., Warchol, A., and Kontinen, K. (2023). Energy Efficiency in Agricultural Production – Experience from Land Consolidation in Poland and Finland. *Energies*, 16(22), 7598. DOI: [10.3390/en16227598](https://doi.org/10.3390/en16227598).
- Binh Duong Statistics Office (2022). *Binh Duong Statistical Yearbook 2021*. Statistical Publishing House. Retrieved May, 2023 from <https://thongke.binhduong.gov.vn/Lists/AnPhamThongKe/DispForm.aspx?ID=23&CategoryId=Ni%20C3%AA%20gi%20C3%A1m%20th%20E1%BB%91ng%20k%20C3%AA%20c%20E1%BA%A5p%20t%20E1%BB%89nh&InitialTabId=Ribbon.Read>.
- Bo, N.V., Hoanh, C.T., Du, P.V. et al. (2019). Adaptation options for agricultural cultivation systems in the South Central Coast under the context of climate change: Assessment Report. CCAFS Working Paper. Retrieved 2023, May from <https://hdl.handle.net/10568/106575>.
- Chatterjee, U., and Majumdar, S. (2022). Impact of land use change and rapid urbanization on urban heat island in Kolkata city: A remote sensing based perspective. *J. Urban Manag.*, 11(1), 59–71. DOI: [10.1016/j.jum.2021.09.002](https://doi.org/10.1016/j.jum.2021.09.002).
- Chughtai, A.H., Abbasi, H., and Karas, I.R. (2021). A review on change detection method and accuracy assessment for land use land cover. *Remote Sens. Appl.: Soc. Environ.*, 22, 100482. DOI: [10.1016/j.rsase.2021.100482](https://doi.org/10.1016/j.rsase.2021.100482).
- Dash, P., Sanders, S.L., Parajuli, P. et al. (2023). Improving the Accuracy of Land Use and Land Cover Classification of Landsat Data in an Agricultural Watershed. *Remote Sens.*, 15(16), 4020. DOI: [10.3390/rs15164020](https://doi.org/10.3390/rs15164020).

- Dutta, D., Rahman, A., Paul, S.K. et al. (2021). Impervious surface growth and its inter-relationship with vegetation cover and land surface temperature in peri-urban areas of Delhi. *Urban Clim.*, 37, 100799. DOI: [10.1016/j.uclim.2021.100799](https://doi.org/10.1016/j.uclim.2021.100799).
- Fisher, R.A., and Koven, C.D. (2020). Perspectives on the future of land surface models and the challenges of representing complex terrestrial systems. *J. Adv. Model. Earth Syst.*, 12(4), e2018MS001453. DOI: [10.1029/2018MS001453](https://doi.org/10.1029/2018MS001453).
- Florim, I., Albert, B., and Shpejtım, B. (2021). Measuring UHI using Landsat 8 OLI and TIRS data with NDVI and NDBI in Municipality of Prishtina. *Disaster Adv.*, 14, 25–36.
- Foody, G.M. (2020). Explaining the unsuitability of the kappa coefficient in the assessment and comparison of the accuracy of thematic maps obtained by image classification. *Remote Sens. Environ.*, 239, 111630. DOI: [10.1016/j.rse.2019.111630](https://doi.org/10.1016/j.rse.2019.111630).
- Fox, J., and Vogler, J.B. (2005). Land-use and land-cover change in montane mainland southeast Asia. *Environ. Manag.*, 36, 394–403. DOI: [10.1007/s00267-003-0288-7](https://doi.org/10.1007/s00267-003-0288-7).
- Gadal, S., and Gloaguen, T. (2023). *Monitoring Land Cover Change in the Southeastern Baltic Sea Since the 1980s by Remote Sensing*. In: S. Niculescu (Ed.) *European Spatial Data for Coastal and Marine Remote Sensing*. Springer, Cham, 59–79. DOI: [10.1007/978-3-031-16213-8_4](https://doi.org/10.1007/978-3-031-16213-8_4)
- Gozdowski, D., Źukovskis, J., Razinkovas-Baziukas, A. et al. (2022). Land cover changes in selected areas next to lagoons located on the southern coast of the Baltic Sea, 1984–2021. *Sustainability*, 14(4), 2006. DOI: [10.3390/su14042006](https://doi.org/10.3390/su14042006).
- Hanh, H.Q., Azadi, H., Dogot, T. et al. (2017). Dynamics of agrarian systems and land use change in North Vietnam. *Land Degrad. Dev.*, 28(3), 799–810. DOI: [10.1002/ldr.2609](https://doi.org/10.1002/ldr.2609).
- Heredia-R, M., Torres, B., Cabrera-Torres, F. et al. (2021). Land Use and Land Cover Changes in the Diversity and Life Zone for Uncontacted Indigenous People: Deforestation Hotspots in the Yasunı Biosphere Reserve, Ecuadorian Amazon. *Forests*, 12(11), 1539. DOI: [10.3390/f12111539](https://doi.org/10.3390/f12111539).
- Islami, F.A., Tarigan, S.D., Wahjunie, E.D. et al. (2022). Accuracy assessment of land use change analysis using Google Earth in Sadar Watershed Mojokerto Regency. *IOP Conf. Ser.: Earth Environ. Sci.*, 950(1), 012091. DOI: [10.1088/1755-1315/950/1/012091](https://doi.org/10.1088/1755-1315/950/1/012091).
- Kovyazin, V.F., Lepikhina, O.Y., Demidova, P.M. et al. (2023). Problems of Forest Resource Management in the Arctic Zone of the Russian Federation. *Lesnoy Zhurnal*, 3, 185–194. DOI: [10.37482/0536-1036-2023-3-185-194](https://doi.org/10.37482/0536-1036-2023-3-185-194).
- Kumari, M., Sarma, K., and Sharma, R. (2019). Using Moran’s I and GIS to study the spatial pattern of land surface temperature in relation to land use/cover around a thermal power plant in Singrauli district, Madhya Pradesh, India. *Remote Sens. Appl.: Soc. Environ.*, 15, 100239. DOI: [10.1016/j.rsase.2019.100239](https://doi.org/10.1016/j.rsase.2019.100239).
- Lemenkova, P., and Debeir, O. (2023). Multispectral Satellite Image Analysis for Computing Vegetation Indices by R in the Khartoum Region of Sudan, Northeast Africa. *J. Imaging*, 9(5), 98. DOI: [10.3390/jimaging9050098](https://doi.org/10.3390/jimaging9050098).
- Lenzen, M., Wier, M., Cohen, C. et al. (2006). A comparative multivariate analysis of household energy requirements in Australia, Brazil, Denmark, India and Japan. *Energy*, 31(2–3), 181–207. DOI: [10.1016/j.energy.2005.01.009](https://doi.org/10.1016/j.energy.2005.01.009).
- Majeed, M., Tariq, A., Anwar, M.M. et al. (2021). Monitoring of land use–Land cover change and potential causal factors of climate change in Jhelum district, Punjab, Pakistan, through GIS and multi-temporal satellite data. *Land*, 10(10), 1026. DOI: [10.3390/land10101026](https://doi.org/10.3390/land10101026).
- Malinowski, R., Lewinski, S., Rybicki, M. et al. (2020). Automated production of a land cover/use map of Europe based on Sentinel-2 imagery. *Remote Sen.*, 12(21), 3523. DOI: [10.3390/rs12213523](https://doi.org/10.3390/rs12213523).
- Mehdi, S.M., Pant, N.C., Saini, H.S. et al. (2016). Identification of palaeochannel configuration in the Saraswati River basin in parts of Haryana and Rajasthan, India, through digital remote sensing and GIS. *Episodes J. Int. Geosci.*, 39(1), 29–38. DOI: [10.18814/epiiugs/2016/v39i1/89234](https://doi.org/10.18814/epiiugs/2016/v39i1/89234).

- Mingarro, M., and Lobo, J.M. (2023). European National Parks protect their surroundings but not everywhere: A study using land use/land cover dynamics derived from CORINE Land Cover data. *Land Use Policy*, 124, 106434. DOI: [10.1016/j.landusepol.2022.106434](https://doi.org/10.1016/j.landusepol.2022.106434).
- Moharram, M.A., and Sundaram, D.M. (2023). Land Use and Land Cover Classification with Hyperspectral Data: A comprehensive review of methods, challenges and future directions. *Neurocomp.*, 536, 90–113. DOI: [10.1016/j.neucom.2023.03.025](https://doi.org/10.1016/j.neucom.2023.03.025).
- Motlagh, Z.K., Lotfi, A., Pourmanafi, S. et al. (2020). Spatial modeling of land-use change in a rapidly urbanizing landscape in central Iran: Integration of remote sensing, CA-Markov, and landscape metrics. *Environ. Monit. Assess.*, 192, 1–19. DOI: [10.1007/s10661-020-08647-x](https://doi.org/10.1007/s10661-020-08647-x).
- Msofe, N.K., Sheng, L., and Lyimo, J., (2019). Land use change trends and their driving forces in the Kilombero Valley Floodplain, Southeastern Tanzania. *Sustainability*, 11(2), 505. DOI: [10.3390/su11020505](https://doi.org/10.3390/su11020505).
- Niu, X., Hu, Y., Lei, Z. et al. (2022). Temporal and Spatial Evolution Characteristics and Its Driving Mechanism of Land Use/Cover in Vietnam from 2000 to 2020. *Land*, 11(6), 920. DOI: [10.3390/land11060920](https://doi.org/10.3390/land11060920).
- Pal, S., and Ziaul, S.K. (2017). Detection of land use and land cover change and land surface temperature in English Bazar urban centre. *Egypt. J. Remote Sens. Space Sci.*, 20(1), 125–145. DOI: [10.1016/j.ejrs.2016.11.003](https://doi.org/10.1016/j.ejrs.2016.11.003).
- Právělie, R. (2018). Major perturbations in the Earth's forest ecosystems. Possible implications for global warming. *Earth-Sci. Rev.*, 185, 544–571. DOI: [10.1016/j.earscirev.2018.06.010](https://doi.org/10.1016/j.earscirev.2018.06.010).
- Rajkhowa, S., Khanom, N.A., and Sarma, J. (2021). *Environmental issues and priority areas for ecological engineering initiatives*. In Handbook of Ecological and Ecosystem Engineering, 47–66. DOI: [10.1002/9781119678595.ch3](https://doi.org/10.1002/9781119678595.ch3).
- Regasa, M.S., Nones, M., and Adeba, D. (2021). A review on land use and land cover change in Ethiopian basins. *Land*, 10(6), 585. DOI: [10.3390/land10060585](https://doi.org/10.3390/land10060585).
- Rimal, B., Zhang, L., Stork, N. et al. (2018). Urban expansion occurred at the expense of agricultural lands in the Tarai region of Nepal from 1989 to 2016. *Sustainability*, 10(5), 1341. DOI: [10.3390/su10051341](https://doi.org/10.3390/su10051341).
- Rivière, F., Widad, F.Z., Speyer, E. et al. (2018). Reliability and validity of the French version of the global physical activity questionnaire. *J. Sport Health Sci.*, 7(3), 339–345. DOI: [10.1016/j.jshs.2016.08.004](https://doi.org/10.1016/j.jshs.2016.08.004).
- Rouse, J.W., Haas, R.H., Schell, J.A. et al. (1973). *Monitoring vegetation systems in the great plains with ERTS*. In C. Freden and M.A. Becker (Eds.) Third Earth Resources Technology Satellite–1 Symposium. Washington DC: National Aeronautics and Space Administration, 1, 309–317.
- Rousta, I., Olafsson, H., Moniruzzaman, M. et al. (2020). Impacts of drought on vegetation assessed by vegetation indices and meteorological factors in Afghanistan. *Remote Sens.*, 12(15), 2433. DOI: [10.3390/rs12152433](https://doi.org/10.3390/rs12152433).
- Rustiadi, E., Pravitasari, A.E., Setiawan, Y. et al. (2021). Impact of continuous Jakarta megacity urban expansion on the formation of the Jakarta-Bandung conurbation over the rice farm regions. *Cities*, 111, 103000. DOI: [10.1016/j.cities.2020.103000](https://doi.org/10.1016/j.cities.2020.103000).
- Singh, S.K., Srivastava, P.K., Gupta, M. et al. (2014). Appraisal of land use/land cover of mangrove forest ecosystem using support vector machine. *Environ. Earth Sci.*, 71(5), 2245–2255. DOI: [10.1007/s12665-013-2628-0](https://doi.org/10.1007/s12665-013-2628-0).
- Singh, P., Sarkar Chaudhuri, A., Verma, P. et al. (2022). Earth observation data sets in monitoring of urbanization and urban heat island of Delhi, India. *Geomat. Nat. Hazards Risk*, 13(1), 1762–1779. DOI: [10.1080/19475705.2022.2097452](https://doi.org/10.1080/19475705.2022.2097452).
- Slamet, B., Syahputra, O.K.H., Kurniawan, H. et al. (2021). Analysis of vegetation cover and built-up areas in the Percut watershed landscape, North Sumatra Province using sentinel-2 imagery. *IOP Conf. Ser.: Earth Environ. Sci.*, 912(1), 012089. DOI: [10.1088/1755-1315/912/1/012089](https://doi.org/10.1088/1755-1315/912/1/012089).
- Sokolov, A., Veselitskaya, N., Carabias, V. et al. (2019). Scenario-based identification of key factors for smart cities development policies. *Technol. Forecast. Soc. Change*, 148, 119729. DOI: [10.1016/j.techfore.2019.119729](https://doi.org/10.1016/j.techfore.2019.119729).

- Surya, B., Salim, A., Hernita, H. et al. (2021). Land use change, urban agglomeration, and urban sprawl: A sustainable development perspective of Makassar City, Indonesia. *Land*, 10(6), 556. DOI: [10.3390/land10060556](https://doi.org/10.3390/land10060556).
- Theres, B.L., and Selvakumar, R., (2022). Comparison of landuse/landcover classifier for monitoring urban dynamics using spatially enhanced landsat dataset. *Environ. Earth Sci.*, 81(5), 142. DOI: [10.1007/s12665-022-10242-x](https://doi.org/10.1007/s12665-022-10242-x).
- Thien, B.B., Sosamphanh, B., Yachongtou, B. et al. (2022). Land use/land cover changes in the period of 2015–2020 in AngYai Village, Sikhottabong District, Vientiane Capital, Lao PDR. *Geol. Geophys. Environ.*, 48(3), 279–286. DOI: [10.7494/geol.2022.48.3.279](https://doi.org/10.7494/geol.2022.48.3.279).
- Thien, B.B., and Phuong, V.T. (2023). Using Landsat satellite imagery for assessment and monitoring of long-term forest cover changes in Dak Nong province, Vietnam. *Geogr. Pannonica*, 27(1), 69–82. DOI: [10.5937/gp27-41813](https://doi.org/10.5937/gp27-41813).
- Thien, B.B., Phuong, V.T., and Komolafe, A.A. (2023a). Assessment of forest cover and forest loss using satellite images in Thua Thien Hue province, Vietnam. *AUC Geogr.*, 58(2), 172–186. DOI: [10.14712/23361980.2023.13](https://doi.org/10.14712/23361980.2023.13).
- Thien, B.B., Yachongtou, B., and Phuong, V.T., (2023b). Long-term monitoring of forest cover change resulting in forest loss in the capital of Luang Prabang province, Lao PDR. *Environ. Monit. Assess.*, 195(8), 1–17. DOI: [10.1007/s10661-023-11548-4](https://doi.org/10.1007/s10661-023-11548-4).
- Vadrevu, K., Heinimann, A., Gutman, G. et al. (2019). Remote sensing of land use/cover changes in South and Southeast Asian Countries. *Int. J. Digit. Earth*, 12(10), 1099–1102. DOI: [10.1080/17538947.2019.1654274](https://doi.org/10.1080/17538947.2019.1654274).
- Verma, P., Raghubanshi, A., Srivastava, P.K. et al. (2020). Appraisal of kappa-based metrics and disagreement indices of accuracy assessment for parametric and nonparametric techniques used in LULC classification and change detection. *Model. Earth Syst. Environ.*, 6, 1045–1059. DOI: [10.1007/s40808-020-00740-x](https://doi.org/10.1007/s40808-020-00740-x).
- Wahla, S.S., Kazmi, J.H., and Tariq, A. (2023). Mapping and monitoring of spatio-temporal land use and land cover changes and relationship with normalized satellite indices and driving factors. *Geol. Ecol. Landsc.*, 1–17. DOI: [10.1080/24749508.2023.2187567](https://doi.org/10.1080/24749508.2023.2187567).
- Waiyasusri, K. (2021). Monitoring the land cover changes in mangrove areas and urbanization using normalized difference vegetation index and normalized difference built-up index in Krabi Estuary Wetland, Krabi province, Thailand. *Appl. Environ. Res.*, 43(3), 1–16. DOI: [10.35762/AER.2021.43.3.1](https://doi.org/10.35762/AER.2021.43.3.1).
- Wiatkowska, B., Słodczyk, J., and Stokowska, A., (2021). Spatial-temporal land use and land cover changes in urban areas using remote sensing images and GIS analysis: The case study of Opole, Poland. *Geosci.*, 11(8), 312. DOI: [10.3390/geosciences11080312](https://doi.org/10.3390/geosciences11080312).
- Wu, Z., Xiong, K., Zhu, D. et al. (2022). Revelation of coupled ecosystem quality and landscape patterns for agroforestry ecosystem services sustainability improvement in the karst desertification control. *Agric.*, 13(1), 43. DOI: [10.3390/agriculture13010043](https://doi.org/10.3390/agriculture13010043).
- Zadbagher, E., Becek, K., and Berberoglu, S. (2018). Modeling land use/land cover change using remote sensing and geographic information systems: case study of the Seyhan Basin, Turkey. *Environ. Monit. Assess.*, 190, 1–15. DOI: [10.1007/s10661-018-6877-y](https://doi.org/10.1007/s10661-018-6877-y).
- Zheng, Y., Tang, L., and Wang, H. (2021). An improved approach for monitoring urban built-up areas by combining NPP-VIIRS nighttime light, NDVI, NDWI, and NDBI. *J. Clean. Prod.*, 328, 129488. DOI: [10.1016/j.jclepro.2021.129488](https://doi.org/10.1016/j.jclepro.2021.129488).